Practical measurement of cell-phone camera lens focal length

Milster, Tom, Kuhn, William

Tom D. Milster, William P. Kuhn, "Practical measurement of cell-phone camera lens focal length," Proc. SPIE 11488, Optical System Alignment, Tolerancing, and Verification XIII, 1148807 (20 August 2020); doi: 10.1117/12.2570622

SPIE.

Event: SPIE Optical Engineering + Applications, 2020, Online Only

Practical measurement of cell-phone camera lens focal length

Tom D. Milster*[a] and William P. Kuhn[b]
[a]College of Optical Sciences, 1630 East University, University of Arizona, Tucson, AZ, USA 85721; [b]Opt-E, 8987 E. Tanque Verde Rd. Ste 309 PMB 270, Tucson, Arizona, USA 85749-9399

ABSTRACT

A practical instrumentation configuration for measuring focal length of cell-phone camera lenses is presented that uses a custom autocollimator, a grating, an autostigmatic microscope, and a precision stage. Uncertainty in LED wavelength is reduced by using a white LED and a set of narrow-band filters. The autocollimator is designed to allow for rapid focus adjustment at each test wavelength. Examples of the measurement technique and an error analysis are provided.

Keywords: Focal length measurement, miniature lenses, cell-phone camera

1. INTRODUCTION

Techniques for measuring lens focal length are numerous.[1-6] Typical measurement precision is ~1%, with precise methods reaching 0.01%. Most of these methods have been developed for lens diameters greater than 1 cm. Measuring the effective focal length (EFL) of small lens systems, like those found in cell phone cameras, is a non-trivial task. Although interferometry has been suggested for miniature lenses,[7] a simple non-interferometric method is preferred for flexibility and ease of operation. In this presentation, we discuss an experimental configuration using a custom autocollimator and an autostigmatic microscope (Opt-E, W2-AM) for this measurement. A goal of this work is to develop a simple test method with ~ 1% accuracy and repeatability.

The following sections discuss a short background of cell-phone camera lenses, characteristics of focal length and effective focal length in complex lenses, the basic measurement philosophy, a detailed discussion of measurement hardware, sources of error, example measurements, and a short discussion of conclusions.

2. BACKGROUND

2.1 Cell-phone camera modules

Cell phones are now a ubiquitous part of our society. An attractive feature of cell phones is the ability to take photographs. Due to the popularity of this feature, cell-phone cameras have evolved into multiple-purpose devices that take high-quality photographs in almost any situation. Instead of carrying three different cameras, an individual with a cell phone can now take photos like a normal camera, a telephoto camera, or a wide-angle camera.

Since different kinds of cameras (telephoto, normal, and wide angle) require different lenses, small, compact cell phones must include different lenses to have different photographic effects. Because it is inconvenient to mechanically change lenses, cell phones contain multiple complete camera systems. For example, the iPhone 11 Pro contains a telephoto camera, a wide-angle camera and an ultra-wide camera. Each of the cameras is a complete camera system, including a lens and an image sensor for collecting images.

Figure 1 illustrates how a cell phone camera takes an image and how the image is displayed on the front face of the camera. The example contains two rear-facing cameras. The telephoto (TELE) camera contains a lens barrel and an image sensor, along with other parts. The lens barrel is the image-forming part of the camera. It forms an image of the object at the image sensor. The image sensor converts the image into electrical signals, which are then sent to a computer inside the phone. The computer receives the signals and displays the image on the front side of the phone.

Optical System Alignment, Tolerancing, and Verification XIII, edited by José Sasián, Richard N. Youngworth, Proc. of SPIE Vol. 11488, 1148807 · © 2020 SPIE
CCC code: 0277-786X/20/$21 · doi: 10.1117/12.2570622

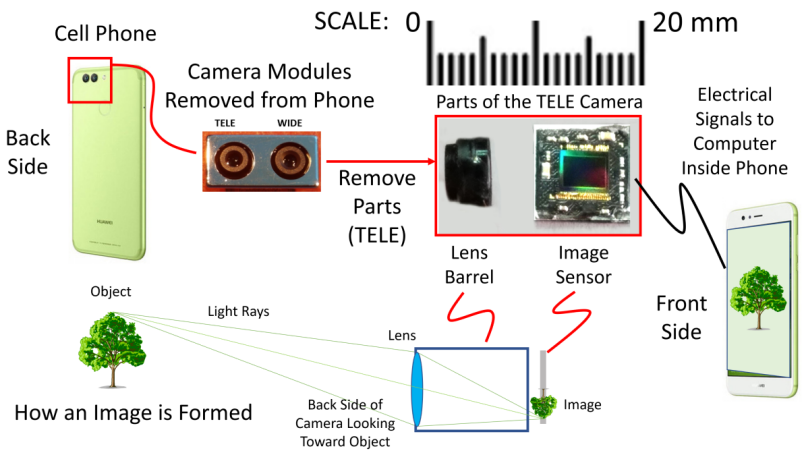

Fig. 1 Cell-phone camera modules are each independent optical systems, including a lens to form the image and a sensor that records the image. The image is usually displayed on the front side of the cell phone.

A simple diagram of a camera module is shown expanded in Fig. 2.[1] The lens barrel fits inside a voice-coil motor (VCM), which contains coil-magnet pairs for focus control. A thin, plane filter glass (IR Cut Filter) is between the VCM and the image sensor. The filter makes the image recoded on the image sensor look more natural to the human eye, because the image sensor is sensitive to infrared (IR) light that the eye cannot see. The complementary metal–oxide–semiconductor (CMOS) image sensor detects the image, as explained above, and the flat printed circuit (FPC) cable communicates electric signals from the image sensor to the computer inside the camera body through a connector.

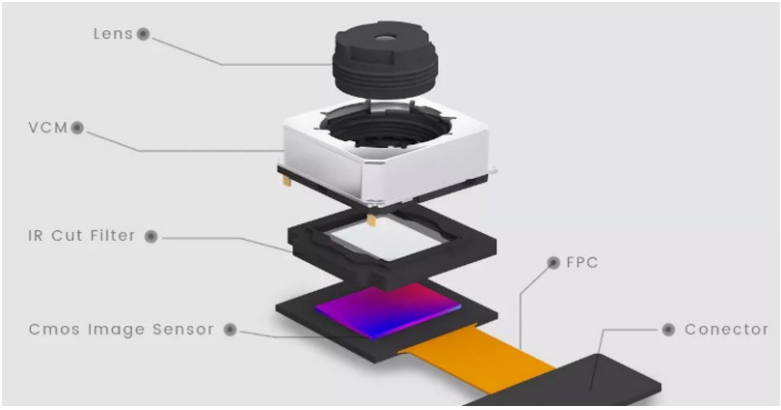

Fig. 2. Diagram of a camera module.[1]

Like in high-quality camera lenses in professional cameras, cell-phone camera lens barrels contain more than one lens element, as shown by the cross section of a Nova 2+ telephoto lens in Fig. 3. The additional lens elements improve image quality, given the ultra-compact volume in which the camera must operate.

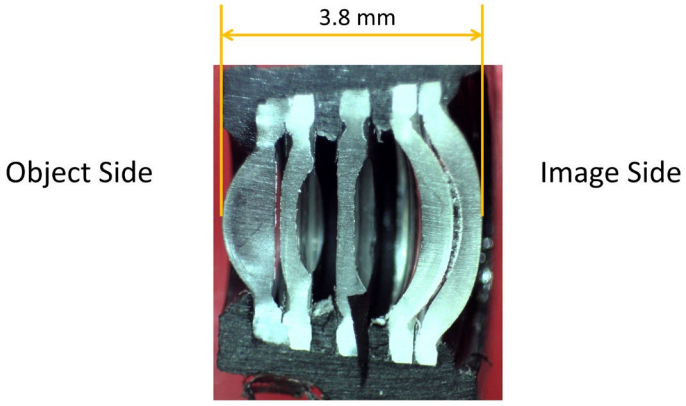

Fig. 3. Cross section of a Nova 2+ cell-phone camera lens module with five optical lens elements.

2.2 Focal length and effective focal length

The focal length measurement is based on a simple principle, as shown in Fig. 4. A parallel ray bundle consisting of light rays 1, 2, and 3 from a distant object is shown incident on a lens element at angle θ, where θ is measured between light ray 3 and the optical axis of the lens element. The rays focus to an image height given by h' = f tan(θ), where in this case the light rays originated from the uppermost object point on the tree. If the angle θ and h' are known, the effective focal length (EFL) f is

$$f = h'/\tan(\theta) \quad . \tag{1}$$

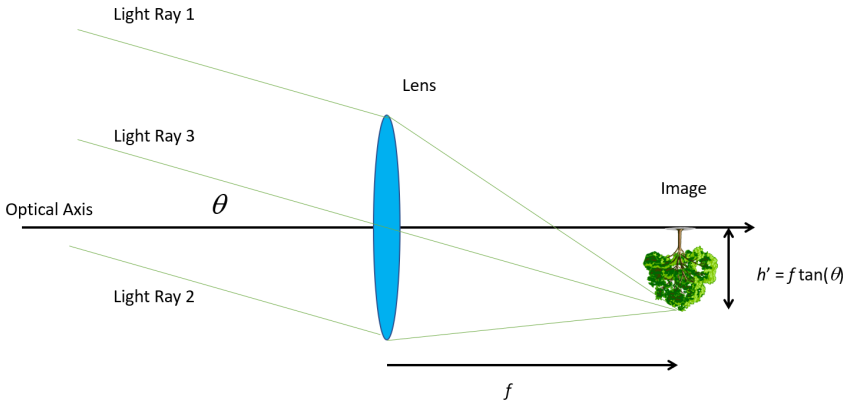

Fig. 4 Relationship used in the calculation of EFL.

The simplified drawing in Fig. 4 conceptually shows a thin lens and the corresponding focal length. However, cell-phone camera lenses are much more complex that a simple thin lens, as shown in Fig. 3, and EFL for these assemblies are not straightforward to calculate based on a simple measurement of the distance between the lens and the image lane. As shown in Fig 5 below,[2] the EFL of a two-lens assembly is adjusted from the position of the last lens to reference the system rear principle plane. However, even in complicated multiple-lens assemblies, like those used in cell-phone cameras, Eq. (1) is valid in regions of the focal plane without significant distortion.

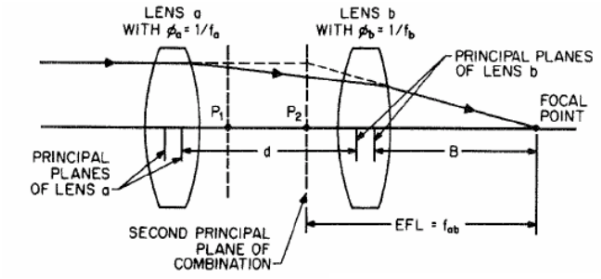

Fig. 5. When an optical system consists of multiple thick lenses, the effective focal length must be adjusted from the vertex of the last lens.[2]

3. MEASUREMENT

3.1 Basic measurement philosophy

Parallel light rays from three known directions are used in the measurement setup. As shown in Fig. 7, a grating is used to produce three ray bundles from each input ray bundle. Each ray bundle out of the grating focuses to a different position in the focal plane of the test lens, as determined by Eq. (1) with a total separation of 2*h*'.

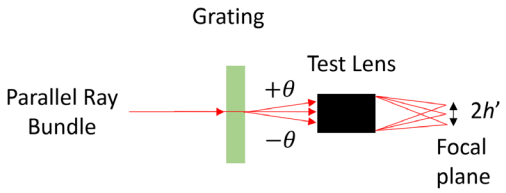

Fig. 6. A grating produces three ray bundles for each parallel ray bundle incident upon it, and these ray bundles are focused at the back focal plane of the lens. The two outermost foci are separated by 2*h*'.

In the experimental setup, a grating is illuminated by a collimated light beam, as shown in Fig. 7. Transmission through the grating produces three ray bundles at angles $+\theta$, 0, and $-\theta$, , and the measurement of 2*h*' is the image height corresponding to the distance between the two outer objects. The 0-angle ray bundle is parallel to the optical axis and is not used in the measurement. The distance 2*h*' is measured with a translating microscope on a precision stage, and EFL is found from

$$f = 2h'/2\tan(\theta) . \qquad (2)$$

This measurement is applied to both individual lens elements and lens modules without filter glass to find effective focal length (EFL).

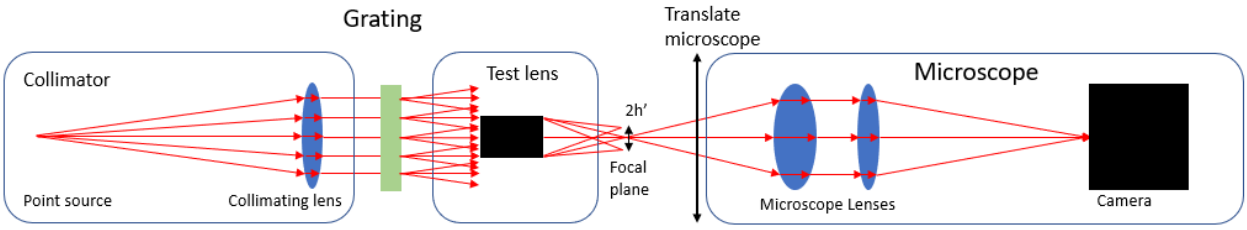

Fig. 7. Conceptual experimental layout

3.2 Measurement hardware

The detailed measurement setup is comprised of the following subsystems:

1. Collimator
2. Grating and mount
3. Test lens and mount
4. Microscope and stages

3.2.1 Collimator

The collimator layout is shown in Fig. 8. The collimator has a point source and collimating lens. As illustrated below, the collimator also has an illumination arm, camera arm, collimator arm and a beam splitter to connect all three parts.

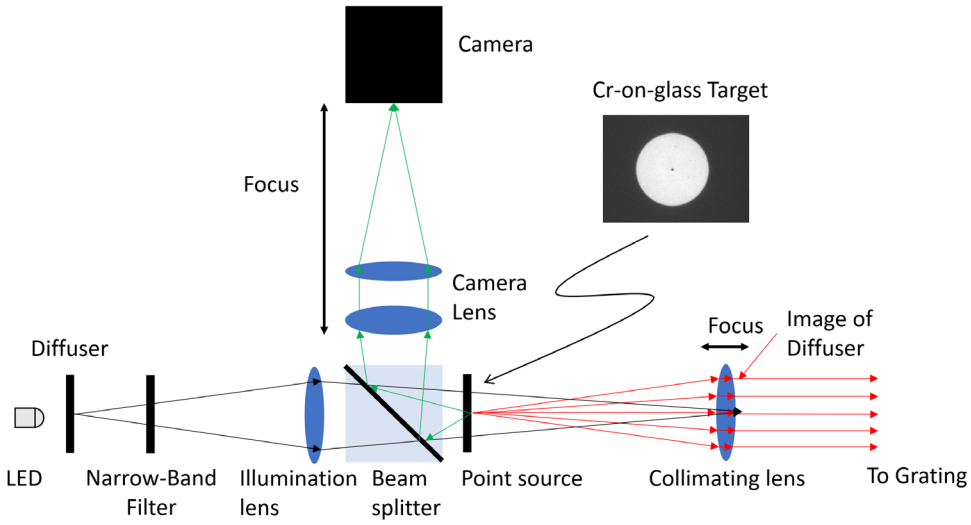

Fig. 8. Layout of the collimator.

The collimator must produce a low aberration wavefront at any of the desired measurement wavelengths. A beam size of 10 mm diameter is substantially larger than the cell-phone camera lenses, which simplifies instrument setup and alignment. An even larger beam diameter has benefits for collimator setup as described below.

A simple way to control a source wavelength with low wavelength uncertainty is to use a broad-spectrum source and narrow band filters. We used Opt-E's current source driver board to drive a white 5mm diameter LED source and incorporated interchangeable narrow band filters in the illumination arm of the collimator. The LED is followed by a diffuser that is the source of the illumination system. The illumination lens projects an image of the diffuser into the exit aperture of the collimator. The filter is placed between the diffuser and illumination space to limit angles of incidence of the light on the filter.

A point source is desired to provide a small artifact for finding a repeatable best-focus position. However, if the only light in the image is from a single source point, it can be difficult to find in a camera image when the point is not well focused. An extended object helps the user to find initial focus and a point object within the field-of-view provides a target to define best focus. Rather than using a pinhole on an otherwise dark field, a reticle with ~3 mm diameter aperture, a ~100 μm diameter, round obscuration, and a ~10 μm diameter aperture (the pinhole) is used to provide a simple target for the test setup, as shown in Fig. 8. This target provides large features that are easily found to rapidly guide the user to a better focus, and then ultimately best focus by observation of the small obscuration. The smallest feature, which is the pinhole, is used when resolvable.

The collimator lens must be precisely focused. Moreover, changing wavelength with different filters results in small focal shifts of the collimator, which would in turn move the image plane of the lens under test and introduces a bias in the measurements. It is necessary to ensure that the collimator is well collimated at all test wavelengths. The collimator

is an autocollimator with a camera system that can focus on the back of the reticle, and if a mirror is placed in front of the collimator, the camera can see the return image as well.

Collimation is verified and set in this instrument by first focusing the camera on the reticle directly by using the camera focus when there is no mirror in front of the collimator, or there is a beam blocking the mirror. The beam block is removed from the setup and the collimator focus is adjusted so that the camera sees both the direct image and a slightly displaced return image.

When the wavelength is changed the operator can quickly refocus the camera to compensate for its focus change and then adjust collimator focus. These adjustments are slight, but critical to making measurements with good repeatability and low measurement uncertainty.

The collimator is made from mostly catalog parts from Thorlabs, as shown Fig. 9. Most of the tubes are SM1 that are made for 1-inch diameter optics. The camera and collimator lenses are achromatic doublets, and illuminator lenses are singlets. This design approach is malleable to different beam sizes, wavelengths, etc.

(a) (b)

Fig. 9. A) Collimator assembly; and b) cutaway view.

3.2.2 Grating and mount

The Edmund Optics 80 lp/mm Cr-on-glass grating shown in Fig. 7 is large enough that critical alignment to the aperture of the collimator and test lens is not required. However, it is convenient to have some height adjustability and some precision in clocking (rotation of the grating about the optical axis). The clocking adjustment can be used to facilitate alignment of the ±1 diffraction orders to the linear motion of the stage used to measure their displacement in the focal plane of the lens under test. Available, but not optimal, laboratory opto-mechanical hardware was used to mount the grating (e.g. post, post clamp, Kapton tape, etc.).

3.2.3 Test lens and mount

A v-block on a 1.5-inch diameter post was used to hold the test lens. Custom machined or 3D printer fixtures can be made when needed. In this experiment, a simple hard-stop in the v-block with a friction-mount hole in a 1-inch lens holder was adequate to locate and hold the lens. The setup should keep beam paths short, space for hands and access for the microscope objective. It is useful to have tip and tilt of the test lens axis to help align the setup. Available laboratory hardware was used.

3.2.4 Microscope and stages

Opt-E's W2-AM[3], as shown in Fig. 10, was the microscope used to view the test lens image plane. The W2-AM is an autocollimator when no microscope objective is attached, and it is an autostigmatic microscope when an objective is attached. In autostigmatic microscope mode, the W2-AM was used along with a manual stage that moves along the optical axis of the test lens to focus onto images of the reticle, as shown in Fig. 9. There is one image of the reticle for

each of the diffracted orders in the field of view of the microscope objective lens. Only the first three diffracted orders are used to limit the range of the image in the central region, where optical distortion is much less than 1%. Typically, the distance 2*h*' is a few hundred micrometers. The ±1 diffraction orders are less intense than the 0 order, due to differences in diffraction efficiencies of the grating.

It is important that the microscope objective NA is large enough to capture all the rays through the test lens for each field-point. Since the test lenses are probably not telecentric, the ray-angle of incidence must also be considered. The measurement can be performed by calculating the pixel distance between the +1 and -1 orders within one image. However, better accuracy is obtained by operating in a null manner, where an accurate stage (Newport VP-XA) is used to move the W2-AM such that the same pixel is positioned at the center of the +1 diffracted order, and then moved to center on the -1 diffraction order. Using this technique, the motion required from the stage does not require magnification and distortion calibration of the microscope.

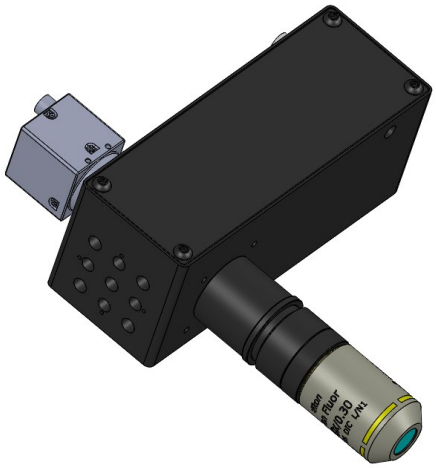

Fig. 10. W2-AM with Nikon objective attached. This is the microscope used to capture images in the focal plane of the test lens.

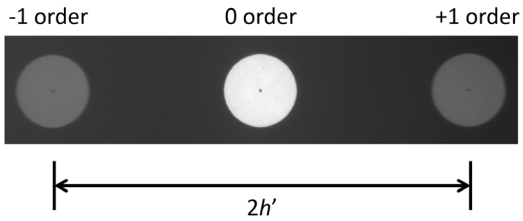

Fig 11. An image through the microscope showing three images of the reticle that correspond to the central three diffraction orders of the grating.

3.3 Sources of error

A simple error analysis based on root-sum-square addition of errors is presented in this section. There are two variables in Eq. (2), so

$$\frac{\delta f}{f} \approx \frac{1}{f}\sqrt{\left(\frac{\partial f}{\partial h'}\Delta h'\right)^2 + \left(\frac{\partial f}{\partial \theta}\Delta\theta\right)^2} \ , \tag{3}$$

where $\Delta h'$ is the error in determining the spacing between the diffracted orders and $\Delta\theta$ is the error in the diffracted angle of each diffracted order. $\Delta h'$ is determined by repeatability of determining ±1 diffracted orders through the microscope as it is translated. A seen from Fig. 11, black dots in centers of the target patterns are very easy to observe, and test results indicate that repeatability is better than $\Delta h'$ = 2 μm.

$\Delta\theta$ is more complicated, where both properties of the light source and the grating are considered. For the two variables,

$$\Delta\theta \approx \sqrt{\left(\frac{\partial\theta}{\partial\lambda}\Delta\lambda\right)^2 + \left(\frac{\partial\theta}{\partial d}\Delta d\right)^2} \ , \tag{4}$$

where d is the grating spacing and λ is the center wavelength of the filter.

The narrow-band filter used (Thorlabs PB530-10) has a catalog center wavelength accuracy of 2 nm and a bandwidth of 10 nm. However, the bandwidth of the filter does not significantly affect spread of the diffracted orders, as observed by the near-circular shape of the round patterns in Fig. 11. The center black dots in the ±1 diffracted orders may be slightly elongated in the direction of dispersion, but the center of the dots can be easily determined by visual inspection. Given the center wavelength accuracy of the grating and assuming a 10% error in locating the center of the dots, the wavelength uncertainty is $\Delta\lambda$ ~ 2.8 nm.

Since

$$\theta = \sin^{-1}\lambda / d \ , \tag{5}$$

$$\Delta\theta \approx \frac{180}{\pi d}\sqrt{\frac{\Delta\lambda^2 + \left(\lambda\frac{\Delta d}{d}\right)^2}{1-\left(\frac{\lambda}{d}\right)^2}} \approx 0.0275° \tag{6}$$

for a d = 12.5 μm period grating (Δd ~ 1%) with λ = 520 nm and $\Delta\lambda$ = 2.8 nm.

With

$$\frac{\partial f}{\partial h'} = \frac{1}{\tan\theta} \ , \tag{7}$$

and

$$\frac{\partial f}{\partial \theta} = \frac{-h'}{\sin^2\theta} \ , \tag{8}$$

a typical value of $\frac{\delta f}{f}$ is about 1% with h' = 0.3 mm and f = 7.5 mm. Precision can be improved by measuring grating spacing, measuring the center wavelength of the bandpass filter, and improving measurement precision of the center dot in the diffraction order. By improving $\Delta\lambda$ to 1 nm and $\Delta h'$ to 0.5 μm, which are reasonable improvements to the procedure, $\frac{\delta f}{f}$ would be ~0.25%.

4. EXAMPLE MEASUREMENTS

A few sample measurements from selected cell phones are shown in Table 1 below. Repeatability of these measurements is better than 1%.

Table 1. Example measurements

Camera Module	2*h*' (mm)	EFL (mm)
Mate 20 Pro TELE	0.632	7.45
Mate 20 Pro Ultra Wide	0.471	5.55
Mi 8 TELE	0.446	5.26
Mi 8 WIDE	0.354	4.17
Nova 2+ TELE	0.471	5.55
Nova 2+ WIDE	0.338	3.98

5. CONCLUSIONS

The test setup used was based on existing prototype and production hardware in our possession and satisfied the schedule, budget, and uncertainty requirements that were needed. The self-referencing autocollimator provided necessary functionality to verify collimation, which was even more important because of the regularly occurring change of operating wavelength. The autocollimator was modified to add narrow band wavelength filters and a precision focusing stage on the output lens. A grating, filters, and a few miscellaneous parts were acquired.

More significant than the self-referencing autocollimator and grating, is the idea that the entire approach can be adapted for measurements made at higher volume, or with even lower uncertainty, or at lower cost. Key to any adaptation is to be sure that the error analysis supports the proposed approach.

For instance, one may measure the image separation 2*h*' directly in a single image, with a different uncertainty and dynamic range than if a stage is used. However, doing so increases uncertainty, unless the image magnification and distortion are calibrated well enough. Additionally, there is a potential cost benefit made possible by eliminating a stage.

One may reduce measurement uncertainty by calibrating the spectrum of the narrow band filters. Whether or not it is worth doing so depends upon the error analysis.

In the end, a rather simple setup allowed for ~1% repeatability and ~1% accuracy at multiple wavelengths.

REFERENCES

[1] Malacara, Optical Shop Testing,, Second Ed., pp.735-737, John Wiley and Sons, Inc., New York, 1992.

[2] B. Howland and A.F. Proll, "Apparatus for the Accurate Determination of Flange Focal Distance," Appl. Opt., pp.1247-1251, 1970.

[3] L.M. Bernardo and O.D.D. Soares, "Evaluation of the Focal Distance of a Lens by Talbot Interferometry." Appl. Opt., pp.296-301, 1988.

[4] Chon-Wen Chang and D.C. Su, "An Improved Method for Measuring the Focal Length of a Lens," Opt. Comm., pp.257-262, 1989.

[5] B.J. Pernick and B. Hyman, "Least Squares Technique for Determining Principal Plane Location and Focal Length." Appl. Opt., 2938-2939, 1987.

[6] DeBoo, B. J., & Sasian, J. M. (2002, December). Novel method for precise focal length measurement. In International Optical Design Conference 2002 (Vol. 4832, pp. 114-121). International Society for Optics and Photonics.

[7] De Angelis, M., De Nicola, S., Ferraro, P., Finizio, A., Pierattini, G., & Hessler, T. (1999). An interferometric method for measuring short focal length refractive lenses and diffractive lenses. Optics communications, 160(1-3), 5-9.

[7] Supertek, “What is a camera module?”, <https://www.supertekmodule.com/what-is-camera-module/> (27 July 2020).

[8] Smith, W. J. (2007). Modern optical engineering 4th edition.

[9] Kuhn, W. P., "Design and performance of a new compact adaptable autostigmatic alignment tool," Proc. SPIE 9951, Optical System Alignment, Tolerancing, and Verification X, 995109 (27 September 2016).